SUSCEPTIBILITY TO ABSORPTION OF ATOMIC HYDROGEN IN API 5L X60 STEELS WITH UNCONVENTIONAL HEAT TREATMENT

D. CALAN-CANCHE [1], *R. GARCÍA-HERNÁNDEZ* [1], *L. DZIB-PÉREZ* [2], *O. L. BILYY* [2], *J. GONZÁLEZ-SÁNCHEZ* [2]

[1] *Metallurgy and Materials Research Institute, Universiudad Michoacana de San Nicolás de Hidalgo, Mexico;*

[2] *Centre for Corrosion Research, Autonomous University of Campeche, Mexico*

Electrochemical behavior of API 5L X60 steel was analyzed in the as-received state and after non-conventional quenching (heated at 1050°C for 30 min and quenched in water) by potentiodynamic polarization and electrochemical impedance spectroscopy in the standard NS4 solution. Samples were potentiostatically hydrogenated for different time in the NS4 solution and the concentration of sub-surface absorbed hydrogen was evaluated by electrochemical oxidation. The heat treated samples absorbed less subsurface hydrogen compared with the base metal due to the presence of more reversible traps in the bainite and acicular ferrite phases. The kinetics of the hydrogen formation was monitored by recording the current which is directly related with the surface changes that occur in the samples tested. The standard deviation of the current in the heat treated steel samples showed the lower values compared to the base metal, which indicates differences in the catalytic activity between the two metallurgical conditions.

Keywords: *atomic hydrogen, heat treatment, standard NS4 solution, resistant to corrosion.*

Corrosion degradation of metallic structures and components affects the infrastructure of all countries: in the environments ranging from deserts to swamps. Corrosion occurs in different environments and its mechanism depends on several factors [1]. One of the methods that minimize the electrochemical corrosion degradation of carbon steel structures is the cathodic protection. In alkaline and neutral environments the cathodic protection of steel structures generates atomic hydrogen by the reduction of water molecules. Carbon steels and other metals are susceptible to hydrogen damage due to the absorption and diffusion of hydrogen through the metal microstructure. The main effects associated with the presence of hydrogen in metals is the modification of mechanical properties and in some cases, the cracks growth and propagation [2, 3].

The whole picture of the interaction processes metal-hydrogen can be described considering three stages: the entry of hydrogen from the surrounding environment into the metal, the transport (diffusion) of hydrogen inside the metal and the trapping of hydrogen at structural defects and/or formation of hydrides phases [4].

Hydrogen permeation experiments allow calculating the diffusion coefficient that is important for analyzing the effect of hydrogen in metals. This methodology uses two electrochemical cells with the two faces of the same sample, one for the hydrogen absorption and the other for the electrochemical hydrogen oxidation. This technique involves the use of very thin samples because the main purpose is to determine the diffusion coefficient of hydrogen in a specific steel. Nowadays few investigations on the effect of hydrogen under real service conditions have been carried out, normally

Corresponding author: J. GONZÁLEZ-SÁNCHEZ, e-mail: jagonzal@uacam.mx

the permeation tests are carried out at high current densities which do not repre-sent the service conditions to which carbon steel structures are subjected. The effect of cathodic polarization on the hydrogen generation and permeation on X-65 pipeline steel samples exposed to neutral pH NS4 soil simulating solution is assessed. It is found that the hydrogen content is less sensitive to the cathodic potential at short charging times, while at longer charging times the hydrogen content in the steel increases almost linearly with the applied potential [5].

The method of electrochemical oxidation is used to determine the total amount of hydrogen absorbed by pipeline steels under cathodic charging, (hydrogenation) [6]. In this methodology the samples previously subjected to hydrogenation for defined periods of time are anodically polarized in an alkaline solution (0.2 M NaOH), which induces the oxidation of the hydrogen absorbed by the sample. This method for determining the concentration of the sub-surface-absorbed hydrogen has been used successfully by other research groups [7, 8].

The high-strength low-alloy steels present a modest corrosion resistance and optimal mechanical properties due to their chemical composition and the thermomechanical manufacturing process. Showing the importance of fossil fuels in energy generation it is necessary to extend the useful life of steel pipelines and structures. Cathodic protection is the most used method for corrosion protection of steel pipelines. Unfortunately, during application of cathodic protection the atomic hydrogen is generated as a part of the protection process, either by reduction of H^+ ions in acidic media or by reduction of water in oxygen-free basic and neutral aqueous electrolytes [9].

Experimental procedure. The micro-alloyed API 5L X60 steel samples were studied in two metallurgical conditions of the base metal in the as-received state: X60MB steel samples and X60TTnC samples subjected to a non-conventional quenching and heat treatment. The samples (150×20×11 mm) subjected to the non-conventional quenching were heated at 1050°C for 30 min and quenched in water at room temperature. After quenching, the samples surface was mechanically grinded with SiC abrasive paper of 240; 600 and 1200 grit followed by polishing with a diamond paste of 0.5 μm up to a mirror finishing. The samples were washed with distilled water, degreased with acetone and dried with air for the metallographic analysis. To evaluate the electrochemical behaviour of the API 5L X60 steel in two metallurgical conditions, samples of 18×16×9 mm were prepared with the same procedure as the samples for metallography except the polishing step, leaving a working surface area of 1 cm^2. Potentiodynamic polarization (PP) and electrochemical impedance spectroscopy (EIS) tests were carried out at room temperature with an electrochemical analyser Solartron model 1280C using a conventional three electrode electrochemical cell with X60MB and X60TTnC samples as working electrodes, a saturated calomel electrode (SCE) as a reference electrode and a graphite bar as an auxiliary electrode. The PP tests were carried out in the deaerated NS4 solution (pH 6.7) applying a cathodic overpotential of 300 mV and an anodic overpotential of 600 mV, both vs. the open circuit potential (OCP) at a scan rate of 10 mV/min. The chemical composition of the NS4 solution is shown in Table 1.

Table 1. Chemical composition of the NS4 solution (g/l)

$MgSO_4 \cdot 7H_2O$	$CaCl_2 \cdot H_2O$	KCl	$NaHCO_3$
0.131	0.181	0.122	0.483

The standard soil simulating NS4 solution used in the present work, was selected in order to have comparison parameters because this solution had been widely used in

studies on hydrogen damage, hydrogen absorption and stress corrosion cracking [4, 6, 9–15]. The EIS measurements were performed applying an AC potential signal of 10 mV at frequencies from 20000 to 0.1 Hz. The EIS results were analyzed using an equivalent electric circuit that gave the best fitting of the Z'' vs. Z' and $|Z|$ vs. logω data (Nyquist and Bode diagram), respectively. In the present case the impedance results are presented only for the Nyquist diagram. The electrochemical noise (EN) measurements were conducted under potentiostatic control (–200 mV vs. OCP) which can give information about the formation of atomic hydrogen at the samples surface. The EN data were statistically treated and standard deviation of the current fluctuations was determined and analyzed.

The hydrogenation of the samples was conducted by applying a cathodic polarization of 200 mV vs. the OCP in the NS4 solution for different periods of time in a conventional electrochemical cell similar to the one described above. For the electrochemical hydrogen oxidation the hydrogenated samples were subjected to anodic polarization in the 0.2 M NaOH solution. All electrochemical measurements were carried out using a Potentiostat/Galvanostat Solartron model 1285.

The hydrogenation of steel samples involves the reduction reaction of the water molecules in the neutral pH NS4 solution according to the following reaction [9–11]:

$$H_2O + e^- \leftrightarrow H_{ads} + OH^-. \quad (1)$$

The H_{ads} evolved by the reaction of Volmer can form the molecules of H_2 by the chemical reaction of Tafel

$$2H_{ads} \leftrightarrow H_2, \quad (2)$$

or by the electrochemical reaction proposed by Heyrovsky

$$H_{ads} + H_2O + e^- \leftrightarrow H_2 + OH^-, \quad (3)$$

or the adsorbed hydrogen can be absorbed and get into the steel:

$$H_{ads} \leftrightarrow H_{abs}. \quad (4)$$

These reactions take place in the alkaline or neutral solutions in the absence of oxygen.

The application of the cathodic potential (–200 vs. OCP) simulates the cathodic protection conditions to which this type of steel is subjected. The total amount of hydrogen formed on the metal surface can be calculated according to Eq. (5) [13]:

$$Q_H^{ev} = \int_0^{\tau_{exp}} I_{cathodic}(\tau)\, d\tau \quad \text{under} \quad E_{cathodic} = \text{const}. \quad (5)$$

The behavior of the formation kinetics of atomic hydrogen on the surface of the steel samples indicates the influence of the microstructure and at different electroactive fastors presents the metal-electrolyte interface.

The oxidation of H_{abs} was carried out in 0.2 molar NaOH solution by the reaction $H^+ \rightarrow H^+ + e^-$, under constant anodic polarization (170 mV vs. SCE), with this procedure it is ensured that most of the H_{abs} that reaches the surface passes to solution in the form of H^+ ion, being able to measure the process with the associated current density [13–15]. The total amount of H_{abs} absorbed by the metal can be determined by means of the equation:

$$Q_H^{abs} = \int_0^{\tau_{des}} \left[I_H(\tau) - I_{ref}(\tau) \right] d\tau \quad \text{under} \quad E_{anodic} = \text{const}, \quad (6)$$

where $I_H(\tau)$ is the anodic polarization current for the hydrogen-charged test piece; $I_{ref}(\tau)$ is the anodic polarization current for the hydrogen-free specimen.

The concentration of hydrogen was determined by the following equation:

$$C_{\mathrm{H}} = \frac{Q_{\mathrm{H}}^{\mathrm{abs}}}{zFv}, \tag{7}$$

where z is the number of electrons participating in the reaction; F is the Faraday's constant and v is the effective volume of the sample.

Results and discussion. The microstructure of the steel without heat treatment contains polygonal and quasi-polygonal ferrite with the islands the pearlite in a way of bands as shown in Fig. 1*a*. The average grain size of the base metal is 6 μm.

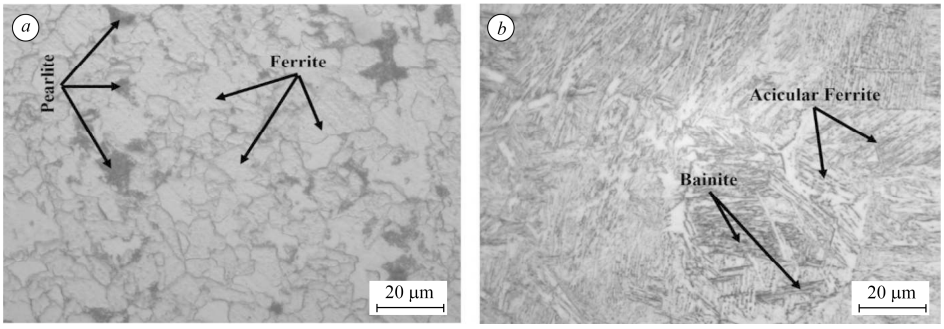

Fig. 1. Microstructure of API 5L X60 steel: *a* – as-received state; *b* – heat treated.

The bainite and acicular ferrite are observed in the heat treated specimens (Fig. 1*b*). The acicular ferrite is defined as a highly sub-structured, non-equiaxed phase that is formed during continuous cooling by a mixed diffusion and shear mode of transformation, beginning at a temperature slightly higher than the upper bainite transformation range [16]. The microstructure formed during the heat treatment gives the better mechanical properties than the initial microstructure due to mainly bainite phase.

Fig. 2 presents the PP curves of the X60MB and X60TTnC steels. The corrosion potentials of these steels are –820 and –770 mV (vs. SCE), respectively. A slight change to the more positive values in the E_{corr} of the heat treated samples, compared with the base metal X60MB, is noticed. The X60MB samples are electrochemically more active in the NS4 solution and present higher corrosion degradation than the samples of the X60TTnC steel. The PP behavior of the X60MB and X60TTnC steels in the standard NS4 solution shows a kinetics, controlled by the charge transfer which indicates that the steel is susceptible to uniform corrosion at a high rate. The X60TTnC samples present a lower corrosion rate than the base metal samples – 0.514 and 0.552 mm/year, respectively. This behavior may be attributed to a rearrangement of grains with a change in the texture during phase transformation in the steel due to the non-conventional quenching which reduces the charge transfer kinetics [12].

Fig. 3 shows the Nyquist diagram for the EIS results of the X60MB and X60TTnC samples in NS4, respectively. This technique allows associating different elements of an equivalent electric circuit to physicochemical processes that occur in the metal-electrolyte interface and identify its electrochemical behavior. The Z'' vs. Z' plot shows a minimal larger charge transfer resistance (R_{ct}) of the X60TTnC sample with respect to the base metal, which corroborates the beneficial effect of the heat treatment.

The EIS values of the elements associated with the equivalent electric circuit listed in Table 2 were simulated using the modified Randles circuit model with the following parameters: R_s is the solution resistance; Q–Y_0 is the constant phase element; Q–n is an exponent; R_{ct} is the charge transfer resistance. The constant phase element (CPE) is mathematically written as:

$$Z_{\mathrm{CPE}} = [Q(j_w)n] - 1. \tag{8}$$

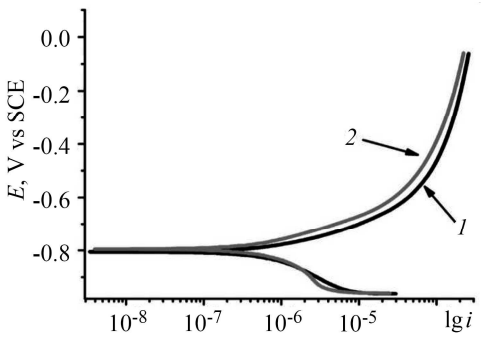

Fig. 2.

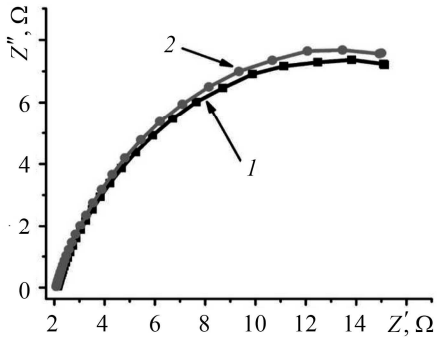

Fig. 3.

Fig. 2. Potentiodynamic polarization curves of the X60MB (curve *1*) and X60TTnC (curve *2*) steels in the NS4 solution.

Fig. 3. Electrochemical impedance spectroscopy of the X60MB (curve *1*) and X60TTnC (curve *2*) steels in the NS4 solution.

Table 2. The equivalent electric circuit elements of the EIS results for the X60MB and X60TTnC steels in the NS4 solution

Steel	R_s, kΩ/cm^2	Q–Y_0, s^n/Ω	Q–n	R_{ct}, kΩ/cm^2
X60MB	21.08	0.000082013	0.76	21748
X60TTnC	20.61	0.000087701	0.77	22019

The mathematical fitting of the parameters shows that the heat treated samples tend to be less susceptible to corrosion (bigger (R_{ct})), compared to the base metal. It has been reported that Q–n is a combination of properties related to the surface and electroactive phenomena [17]. In the present case the increase in the charge transfer resistance observed for the heat treated samples can be attributed to the microstructure modification due to the presence of the bainite and acicular ferrite phases [18].

The EN are fluctuations of potential or current, typically of low-equency (< 10 Hz) and low-amplitude, taking place in the metal–electrolyte (electrified interphase), which can be measured under conditions of open circuit potential or under potentiostatic or galvanostatic control [17]. The EN under potentiostatic and galvanostatic control has been used to interpret the kinetics of corrosive processes of a lange variety of the metal–electrolyte systems including the processes associated with hydrogen evolution [17, 19, 20].

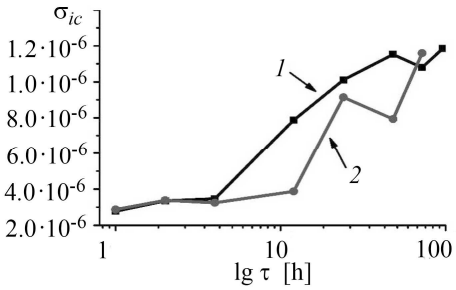

Fig. 4. Standard deviation of the current associated with the evolution of hydrogen in the X60MB (curve *1*) and X60TTnC (curve *2*) steel samples.

Fig. 4 presents a standard deviation of the current signal obtained from the process controlled by the charge transfer and shows an increase, as the rate of the corrosion process increases and the corrosion becomes more localized [20]. The standard deviation of the current signal (σ_{ic}), associated with the production of atomic hydrogen in the X60TTnC and X60MB steels samples tends to increase as a function of the hydrogenation time. The monitoring of σ_{ic} can give information about the kinetics of evolution that is related to the metallurgical condition of the surface hydrogen.

During the first 4 h of hydrogenation the behavior of the tested samples is similar to a small increment of the σ_{ic}, values for the X60TTnC and X60MB samples. A drastic increase of σ_{ic} is observed after 12 h of hydrogenation on the base metal samples, which indicates a greater catalytic activity on the surface. The samples of the heat treated steel show a minimal increase of the current standard deviation, which is related to the lower electrochemical activity than the base metal samples. For the hydrogenation periods larger than 12 h the non-conventional quenched samples show a more noticeable increase of σ_{ic}, but always lower than that for the base metal samples.

Fig. 5 presents the concentration of hydrogen of the X60MB and X60TTnC steels. The amount of electrical charge associated with the sub-surface absorption of atomic hydrogen (Q_H^{abs}), is the area under curve I (A/cm^2) vs. time (s). The cathodic polarization (–200 mV vs. OCP), induces hydrogen absorption in both the X60MB and X60TTnC steels samples, which can promote the diverse forms of hydrogen damage, although at different levels of aggressiveness.

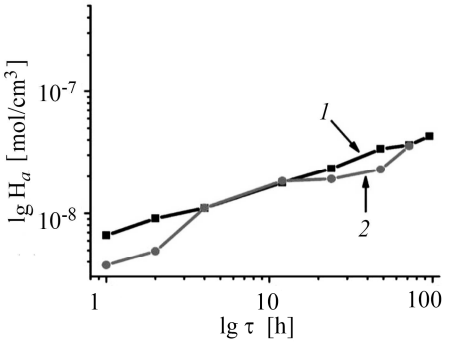

Fig. 5.

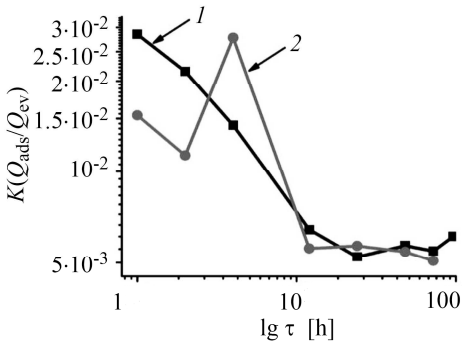

Fig. 6.

Fig. 5. Sub-surface hydrogen concentration in the X60MB (curve *1*) and X60TTnC (curve *2*) steel samples.

Fig. 6. Behavior of the permeation coefficient in the X60MB (curve *1*) and X60TTnC (curve *2*) samples.

In the NS4 solution the X60MB steel shows a higher sub-surface hydrogen absorption compared to the X60TTnC steel during different hydrogenation periods. The sub-surface hydrogen concentration always tends to increase for longer hydrogenation times. The X60TTnC steel samples that present a bainite-acicular ferrite microstructure absorb less hydrogen compared to the non heat-treated steel (Fig. 5, curve *2*) and according to the charge associated with absorbed hydrogen ($Q_{H_{abs}}$).

It was reported that the microstructure comprising acicular ferrite and bainite provides a high quantity of reversible trapping sites and the hydrogen trapping efficiency increases according to the transformation sequence of degenerated perlite, bainite and acicular ferrite, with acicular ferrite being the most efficient [18].

Fig. 6 shows the behavior of the hydrogen permeation coefficient (K) of the X60MB and X60TTnC steels, respectively. With the electrochemical charge associated with the evolution and absorption of hydrogen, the hydrogen permeation efficiency coefficient in the tested samples is calculated: $K = Q_{abs}/Q_{ev}$. This coefficient presents the highest value during the first hours of hydrogenation, however, with increasing hydrogenation time, K decreased. Coefficient K reflects the dynamics of the electrochemical processes at the metal-environment interface. The decrease of this coefficient

with time can be explained by hydrogen saturation of the metal surface above the solubility limit [14].

CONCLUSIONS

The API 5L X60 steel in the two metallurgical conditions studied in this investigation is susceptible to sub-surface absorption of hydrogen in the NS4 solution. The samples without heat treatment are more susceptible to hydrogen absorption as indicated by the higher sub-surface hydrogen concentration, which tends to increase with a longer hydrogenation time.

The microstructure has a significant influence on the susceptibility to sub-surface absorption of atomic hydrogen, since in the test solution the samples with non-conventional heat treatment tend to absorb the lower amount of atomic hydrogen, bainite and acicular ferrite, present in the heat treated samples are characterized by the presence of reversible traps unlike ferrite.

Acicular ferrite and bainite provides a high quantity of reversible trapping sites and the hydrogen trapping efficiency increases according to the transformation sequence of degenerated perlite, bainite and acicular ferrite, with acicular ferrite being the most efficient.

РЕЗЮМЕ. Проаналізовано електрохімічну поведінку сталі API 5L X60 у вихідному стані та після гартування (нагрів до 1050°C упродовж 30 min і охолодження у воді) методом потенціодинамічної поляризації і спектроскопії електрохімічного імпедансу в стандартному розчині NS4. Зразки наводнювали за допомогою потенціостата в розчині NS4, концентрацію поглинутого підповерхневого водню оцінювали, застосовуючи електрохімічне окиснення. Виявили, що зразки після термічної обробки абсорбуються цим воднем менше, ніж у вихідному стані, що зумовлено більшою кількістю реверсивних пасток на бейнітових та ацикулярних феритових фазах. Кінетику формування водню контролювали, реєструючи струм, який безпосередньо пов'язаний зі змінами поверхні. Стандартне відхилення значення струму в гартованих зразках вказало на нижчі його значення проти вихідного металу, а отже, на відмінності каталітичної активності двох металургійних станів.

РЕЗЮМЕ. Проанализировано электрохимическое поведение стали API 5L X60 в исходном состоянии и после закаливания (нагрев до 1050°C в течение 30 min и охлаждение в воде) методом потенциодинамической поляризации и спектроскопии электрохимического импеданса в стандартном растворе NS4. Образцы наводороживали с помощью потенциостата в растворе NS4, концентрацию поглощенного подповерхностного водорода оценивали, применяя электрохимическое окисление. Выявили, что образцы после термической обработки абсорбируются этим водородом меньше, чем в исходном состоянии, вследствие большего количества реверсивных ловушек на бейнитових и ацикулярных ферритных фазах. Кинетику формирования водорода контролировали, регистрируя ток, который непосредственно связан с изменениями поверхности. Стандартное отклонение значений тока в закаленных образцах свидетельствует о более низких значениях по сравнению с исходным металлом, а, следовательно, о различии каталитической активности двух металлургических состояний.

1. *Atmospheric* corrosion of aluminium in the northern Taklamakan Desert environment / S. Sun, Q. Zheng, J. Wen, and D. Li // Mat. and Corr. – 2010. – **61**. – P. 852–859.
2. *Niu L. and Cheng Y. F.* Corrosion behavior of X-70 pipe steel in near-neutral pH solution // Appl. Surf. Sci. – 2007. – **253**. – P. 8626–8631.
3. *Effect* of environmental and metallurgical factors on hydrogen induced cracking of HSLA steels / W. K. Kim, U. K. Boo, Y. Y. Kyoo, and Y. Kim // Corr. Sci. – 2008. – **50**. – P. 3336–3342.
4. *Zakroczymski T.* Adaptation of the electrochemical permeation technique for studying entry, transport and trapping of hydrogen in metals // Electroch. Acta. – 2006. – **51**. – P. 2261–2266.
5. *He D. X., Chen W., and Luo J. L.* Effect of cathodic potential on hydrogen content in a pipeline steel exposed to ns4 near-neutral ph soil solution // Corrosion. – 2004. – **60**. – P. 778–786.

6. *Yan M. and Weng Y.* Study on hydrogen absorption of pipeline steel under cathodic charging // Corr. Sci. – 2006. – **48**. – P. 432–444.
7. *Effect* of hydrogen concentration on fatigue crack growth behaviour in pipeline steel / I. M. Dmytrakh, R. L. Leshchak, A. M. Syrotiuk, and R. A. Barna // Int. J. Hydrogen Energy. – 2017. – **42**. – P. 6401–6408.
8. *Sharifi-Asl S. and Macdonald D. D.* Investigation of the kinetics and mechanism of the hydrogen evolution reaction on copper // J. of Electrochem. Soc. – 2013. – **160**. – P. 382–391.
9. *Dafft E. G., Bohnenkamp K., and Engell H. J.* Investigations of the hydrogen evolution kinetics and hydrogen absorption by iron electrodes during cathodic polarization // Corr. Sci. – 1979. – **19**. – P. 591–612.
10. *Cheng Y. F.* Fundamentals of hydrogen evolution reaction and its implications on near-neutral pH stress corrosion cracking of pipelines // Electrochim. Acta. – 2007. – **52**. – P. 2661–2667.
11. *Cheng Y. F.* Thermodynamically modeling the interactions of hydrogen, stress and anodic dissolution at crack-tip during near-neutral pH SCC in pipelines // J. Mater Sci. – 2007. – **42**. – P. 2701–2705.
12. *Electrochemical* corrosion behavior of the X90 linepipe steel in NS4 solution / J. Luo, L. Zhang, L. Li, F. Yang, W. Ma, K. Wang, and X. Zhao // Natural Gas Industry B. – 2016. – **3**. – P. 346–351.
13. *Sensitivity* of pipelines with steel API X52 to hydrogen Embrittlement / J. Capelle, J. Gilgert, I. Dmytrakh, G. Pluvinage /// Int. J. of Hydrogen Energy. – 2008. – **33**. – P. 7630–7641.
14. *Capelle J., Dmytrakh I., and Pluvinage G.* Comparative assessment of electrochemical hydrogen absorption by pipeline steels with different strength // Corr. Sci. – 2010. – **52**. – P. 1554–1559.
15. *Maocheng Yan, Yongji Weng* Study on hydrogen absorption of pipeline steel under cathodic charging // Corr. Sci. – 2006. – **48**. – P. 432–444.
16. *Coldren A. P. and Mihelich J. L.* Acicular ferrite HSLA steels for line pipe // Metal. Sci. and Heat. Treatment. – 1977. –**19**. – P. 559–572.
17. *Turgoose S., and Cottis R.* Electrochemical impedance and noise. – United States of America: Houston (Tex): NACE, 1999.
18. *Effect* of microstructure on the hydrogen trapping efficiency and hydrogen induced cracking of linepipe steel / G. T. Park, Sung Ung Koh, Hwan Gyo Jung, and Kyoo Young Kim // Corr. Sci. – 2008. – **50**. – P. 1865–1871.
19. *ASTM* Standardization of electrochemical noise measurement, Electrochemical noise measurement for corrosion applications / J. R. Kearns, D. A. Eden, M. R. Yaffe, J. V. Fahey, D. L. Reichert, and D. C. Silverman. – USA: Amer. Soc. for Test. and Mat., 1996. – P. 446–470.
20. *Electrochemical* noise study of the effect of electrode surface wetting on the evolution of electrolytic hydrogen bubbles / H. Bouazaze, S. Cattarin, F. Huet, M. Musiani, and R. Nogueira // J. of Electroanalyt. Chem. – 2006. – **597**. – P. 60–68.

Received 12.06.2018